Journal of Alloys and Compounds 846 (2020) 156351

Contents lists available at ScienceDirect

Journal of Alloys and Compounds

journal homepage: http://www.elsevier.com/locate/jalcom

Application of a natural antioxidant as an efficient strategy to decrease the oxidation in Sn-based perovskites

Hamideh Mohammadian-Sarcheshmeh [a], Mohammad Mazloum-Ardakani [a, *], Mohammad Rameez [b], Saeed Shahbazi [b], Eric Wei-Guang Diau [b]

[a] Department of Chemistry, Faculty of Science, Yazd University, Yazd, 89195-741, Iran
[b] Department of Applied Chemistry and Institute of Molecular Science, National Chiao Tung University, 1001 Ta-Hsueh Rd., Hsinchu, 30010, Taiwan

ARTICLE INFO

Article history:
Received 30 March 2020
Received in revised form
27 June 2020
Accepted 7 July 2020
Available online 18 July 2020

Keywords:
Sn oxidation
Antioxidant
Uric acid
Sn–PSCs

ABSTRACT

This study aims at the application of uric acid (UA), as a natural antioxidant, an inexpensive and available additive, in the fabrication of Sn-perovskite solar cells (Sn–PSCs). First, we fabricate a carbon structure Sn-PSC without the HTM layer which is more economical and environmentally friendly. Then, we investigate the effect of a UA additive on their performance. An important problem in Sn–PSCs is tin oxidation, producing p-type doping and Sn vacancies in the cells. All of these lead to serious device deterioration and low performance. In this case, adding UA helps to improve the photovoltaic parameters and, in particular, the device performance as a result of an effective decrease in Sn^{2+} oxidation and carrier recombination. Also, the device stability improves, in comparison to devices not treated with UA. According to the findings of this study, the UA can replace some expensive additives to prevent tin oxidation and significantly improve photovoltaic parameters.

1. Introduction

The Pb–PSCs have extensively been considered as superior performance PSCs. However, toxicity is a huge barrier to large-scale application and commercialization. Development of Pb–PSCs in which Pb is replaced with less toxic and environmentally friendly metals such as Cu^{2+}, Sn^{2+}, Sb^{3+}, Bi^{3+}or Ge^{2+} can, thus, be a good idea [1–8]. Among those metals, only Sn^{2+} has attracted outstanding attention due to its similarity of electron configuration and coordination geometry to Pb. Sn–PSCs, with the well-known formula of $ASnX_3$, are the best choice to replace Pb. The Sn–PSCs have some advantages such as better carrier mobility than that of Pb–PSCs, better bandgap than that of Pb–PSCs, and low exciton binding energies. Sn–PSCs can supply greater short-circuit current densities (J_{sc}) and a theoretical power conversion efficiency (PCE) about 33% (i.e. Shockley-Quisser limit). Nevertheless, the efficiency of Sn–PSCs is smaller than that of Pb–PSCs, which is explainable for various reasons. In Sn–PSCs, Sn^{2+} will be simply oxidized to Sn^{4+} by a negligible amount of oxygen when Sn–PSCs are exposed to air or inert atmosphere. This phenomenon has been ascribed to the absence of inert pair effects in Sn^{2+}, as compared to Pb^{2+}, creates unwanted high conductivity (p-doping) in perovskite films and thus produces Sn vacancies in perovskite lattices. All this, seriously leads to destroying of cells against the environmental situation. The small formation energy of Sn vacancies increases doped hole concentrations in Sn–PSCs. This, in turn, increases carrier recombination in the PSCs. The reproducibility of Sn–PSCs performance is poor because it is hard to protect these devices against O_2 [9]. Also, the quick reaction between organic ammonium salts and SnI_2 provides some problems in the control of morphology [10]. So far, various strategies have been employed to solve these problems [11,12]. Tin fluoride (SnF_2), as an additive, has been reported to prevent Sn^{2+} oxidization and hole density in Sn–PSCs as well as to increase stability and reproducibility in Sn–PSCs [13]. SnF_2 is a chemically stable Sn^{2+} composition which changes tin perovskite films into Sn^{2+}-rich films and, thus, prevents the formation of Sn vacancies. However, due to agglomeration, a high percentage of SnF_2 can create a separate phase in a perovskite film [14].

In addition to the decrement of Sn^{2+} oxidation, the construction of pinhole-free, well-crystalline, and compact perovskite films are so critical to make enhanced-performance Sn–PSCs. In a Sn-PSC, besides the Sn^{2+} vacancies, dangling bonds at grain boundaries and surface can create trapping states which are as non-radiative recombination regions. This leads to a decrease in device

* Corresponding author.
E-mail address: mazloum@yazd.ac.ir (M. Mazloum-Ardakani).

https://doi.org/10.1016/j.jallcom.2020.156351
0925-8388/

performance. Deep charge trapping states and defects can decrease oxygen penetration routes into their inner domain to oxidize Sn^{2+} [15]. Therefore, proper quality is essential for Sn-perovskite films to inhibit the appearance of those deep charge trapping states and defects and, thus, to increase the cell performance and stability. There are some approaches to the improvement of perovskite film morphology by changing their composition, application some reducing additives [16]. Dimethyl sulfoxide (DMSO), as a precursor, can be used to form a SnI_2: 3 DMSO intermediate phase to restrict the quick crystallization of Sn−PSCs and thus provides homogenous and compact Sn-based perovskite layers [17]. In another approach, a reducing atmosphere of steamed hydrazine can be used to suppress the oxidation and reduce defects and traps which are recombination sites in perovskite films. Some researchers practiced solvent engineering and used a SnF_2-pyrazine complex in this regard. Adding pyrazine enhances the SnF_2 solubility and thus the formamidinium tin triiodide ($FASnI_3$) film quality [18]. Organic cations have also proved to have a substantial role in making Sn−PSCs stable. More stable cells can be achieved when cation MA^+ is substituted by FA^+ to produce a $(MA)_x$ $(FA)_{1\_x}$ SnI_3 cell [19]. Furthermore, it has been shown that the stability of $FASnI_3$ is better than $MASnI_3$ [20]. In the $MASnI_3$ PSCs oxidization of Sn^{2+} is easier. This defect causes quick degradation in air and a remarkable electrical decline of cells. In order to increase stability, decreased dimensional perovskites films (i.e. 2D films) were applied instead of common 3D films. Butylammonium iodide (BAI) was added to $MASnI_3$ to obtain $BA_2MA_{n\_1}SnnI_{3n+1}$ solar cells. This 2D Sn-PSC is more stable than the 3D counterpart (i.e. $MASnI_3$); however, the device performance is lower [21]. Sargent introduced 2D/3D PSCs $(PEA_2\ (FA)_{n-1}\ Sn_n\ I_{3n+1})$ with a superior PCE and increased cell stability [22]. Some studies introduced passivation methods to decrease trap density and to augment moisture-stability [23]. Application of antioxidants can be another method to decrease Sn oxidation and, hence, to improve the cell morphology and efficiency. Feng Yan [24] added an antioxidant, hydroxybenzene sulfonic acid salt, to a perovskite precursor with $SnCl_2$. The reaction of the SO_4^{2-} and the Sn^{2+} ions resulted in the encapsulation of grains in the perovskite layer. This led to supreme oxidation stability in Sn−PSCs. In another work, Mingkui Wang [25] used antioxidant tea polyphenol to Stabilization of $CsPb_{0.5}Sn_{0.5}I_2Br$ perovskite solar cell.

In the present study, uric acid (UA) with different percentages (5%, 10%, and 15%) is used as an additive in perovskite solutions. UA (Scheme 1), a weak acid, serves as a natural antioxidant in the human body fluids to reduce hemoglobin oxidation, inhibit hyaluronic acid oxidation [26], provide stable coordination complexes with Fe ions, and create transition metal ion complexes [27,28]. Some metal complexes were reported interaction between N and C═O groups in UA and some ions such as Pb, Mn, Ni, Cu, Zn, and Co. Experiments have shown that more than one metal UA complex can be synthesized depending on condition employed (pH, stoichiometric ratio, heating, time of heating) [29,30].

We used $FASnI_3$ PSCs due to superior stability [31]. A hole transport material (HTM)-free PSC was employed as a cell with a carbon layer as a cathode (FTO/C−TiO_2 (compact layer)/TiO_2 mesoporous/Al_2O_3 mesoporous/Carbon). Carbon materials have, indeed, been successfully employed as cathodes in HTM-free PSCs to achieve low-cost and simple devices. This has been made possible by eliminating HTM and expensive metals (Ag, Au) [32,33]. Also, carbon materials are inherently hydrophobic, stable, and inactive to ion movements. This feature helps to overcome moisture sensitivity in halide perovskites and increase their stability [34]. For the first time in 1996, Gratzel and co-workers used graphite and carbon black composites instead of noble metal in DSSCs [35]. In 2013, an HTM-free PSC was fabricated with the structure of $TiO_2/ZrO_2/C$ [36]. In our study, the screen printed method is used for the deposition of layers in carbon-based PSCs without HTM. All of the mentioned properties have made our solar cells liable enough for commercialization.

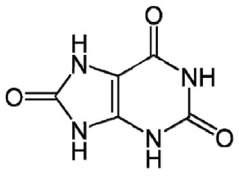

Scheme 1. Uric acid structure.

So far, various methods such as ultraviolet−visible spectroscopy (UV), field-emission scanning electron microscopy (FESEM), X-ray diffraction (XRD), X-ray photoelectron spectroscopy (XPS), Photoluminescence (PL), and I−V curve measurement have been used to investigate different properties of the fabricated cells. By these methods, it has been affirmed that the enhancement of open-circuit voltage (V_{oc}), performance, and stability through the reduction of Sn^{2+}oxidation to Sn^{4+} can decrease the defect states and carrier recombination.

2. Experiments

2.1. Materials

SnI_2 (99.99%, Alfa Aesar), formamidine iodide (99%, Dyesol), TiO_2 paste (Dyesole 18NR-T) and SnF_2 (99%), titanium diisopropoxidebis 75% in iso-propanol, dimethyl sulfoxide (DMSO), dimethylformamide (DMF), and Uric acid (≥99%) from Sigma Aldrich.

2.2. Preparation of devices

A C−TiO_2 layer (50 nm) was deposited on a FTO glass sheet by the spray pyrolysis of a titanium diisopropoxidebis/anhydrous ethanol solution. The glass was later annealed at 450 °C. Then, three layers including mesoporous TiO_2, Al_2O_3, and carbon layers with the thickness 1, 1, and 10 μm were screen printed on the C−TiO_2 layer and sintered at 500 °C, 400 °C, and 400 °C for 30 min, respectively. All pastes were prepared according to previous works [37]. A perovskite precursor solution ($FASnI_3$) was prepared with the equimolar proportions of SnI_2 (1 M) and FAI (1 M) in 0.5 mL DMF: DMSO (50:50) and SnF_2 (0.1 M). The perovskite solution (3 μL) was added to the cell, dried at 70 °C (for 10 min), then annealed at 130 °C (for 10 min) to complete the device fabrication.

2.3. Material characterization

A field-emission scanning electron microscope (FESEM, Hitachi SU8010) was applied to show the structural property of the device. The absorption spectra of the films were provided by a UV−Vis/NIR spectrophotometer with an integrating sphere (V-570, Jasco). Photoluminescence (PL) was carried out by a JASCO monochromator (CT-50TFP, F-number = 4.3, focal length = 500, and grating 600 lines mm^{-1} with a blaze at 1000 nm). The sample was excited by a Q-switched Nd-YAG laser (IB Laser, DiNY pQ532). The repetition rate of the laser was 500 Hz, and its pulse width was 532 nm. The crystal structure in the perovskite film was obtained via X-ray diffraction (XRD, Bruker D8-Advance, with Cu K_α radiation). Through Thermo K-ALPHA Surface Analysis, the X-ray photoelectron spectra (XPS) were investigated for the perovskite samples. The photovoltaic investigations were done with a solar simulator (AM 1.5G, XES-40S1, SAN-EI) which was calibrated with a standard Si reference cell (Oriel, PN 91150V, VLSI standards). A

metal mask with an area of 0.09 cm^2 was utilized in these measurements.

3. Measurements

In the first step, different percentages of UA were added to a $FASnI_3$ solution. Then, the colors of the resulting solutions were compared after the solutions were kept in the environment with the humidity of 65% for 50 min. The results are shown in Fig. 1a and Fig. 1b. As the figures suggest, after 50 min, the yellow $FASnI_3$ solution (0%) turned to red completely, which means the intensive oxidation of Sn in the ambient conditions. However, as can be seen, the change of color in solutions that contained UA (5%, 10%, and 15%) was not so intensive. Therefore, it was expected that the oxidation of Sn decreased when UA was added. It can also be seen that among the solutions with UA, the intensity of color change for solutions with 10% and 15% UA is lower than that of the solution with 5% UA. In this study, an inexpensive carbon counter electrode was used based on Sn-PSC with the construction of FTO/C—TiO_2/TiO_2/Al_2O_3/carbon. This structure is free of organic and inorganic HTMs. Fig. 1c and 1d presents the device structure with different layers.

To confirm the effectiveness of UA, certain measurements were done after the UA was added to the electrode structure. Fig. 2a presents the absorption spectra for the $FASnI_3$ film and the $FASnI_3$ with different percentages of UA (5%, 10%, and 15%). There were no special changes in the wavelengths after the UA was added. However, there was an increase in the absorbance intensities once different percentages of UA were added. These findings imply that UA molecules are not replaced into the tin-perovskite lattice. Also,

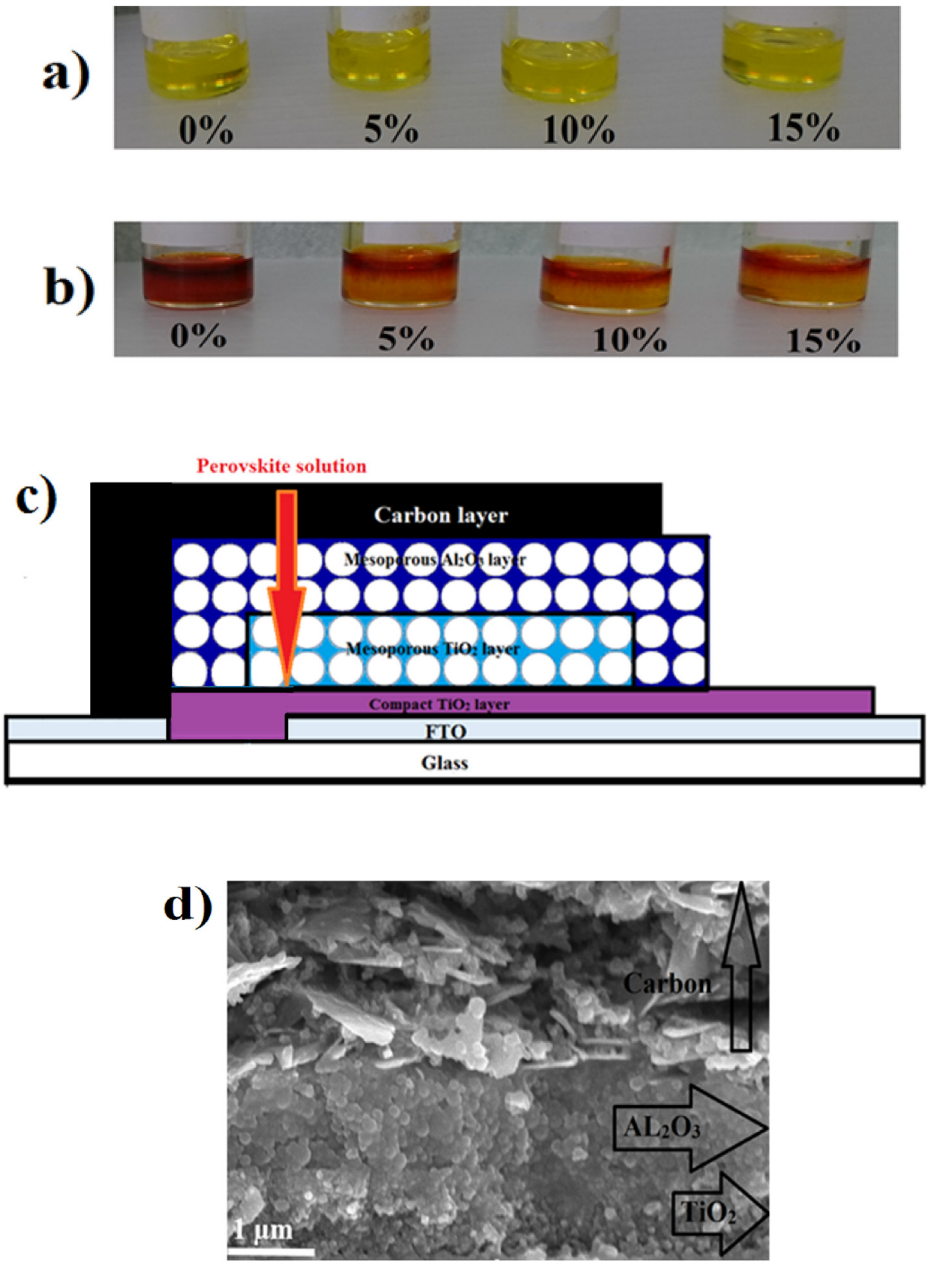

Fig. 1. Comparing of $FASnI_3$ solution with the different percent of UA. a) Starting time and b) 50 min after exposure in ambient (65% Humidity). c) Device structure, and d) SEM image for device structure with TiO_2/Al_2O_3/Carbon layers along with growth perovskite crystals.

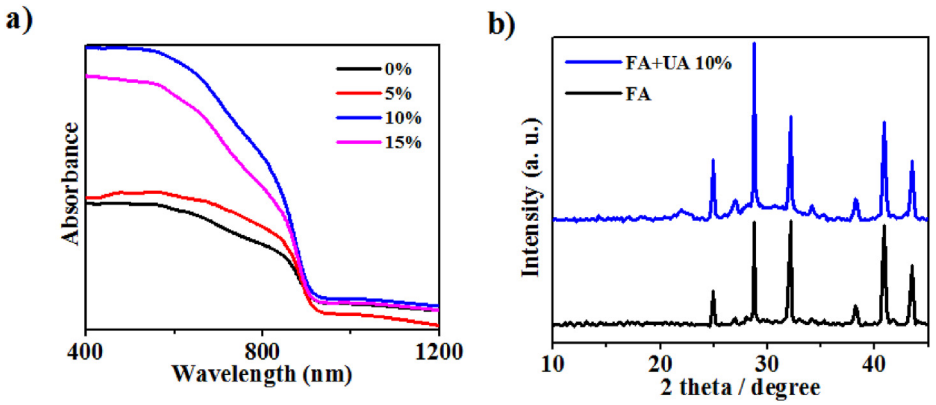

Fig. 2. a) Absorbance for cells with the different percent of UA added to $FASnI_3$ solution. b) XRD patterns of the $FASnI_3$ and $FASnI_3$ with 10% UA.

it seems UA additives can improve the quality and crystallinity of films, which originally has poor morphology as well as defects and deep charge traps caused by Sn oxidation. We considered 10 percent as the optimized amount of UA in this regard. It showed higher absorbance (Fig. 2a) and better stability in the primary tests (Fig. S1).

The variation of crystallinity was investigated by XRD. Fig. 2b illustrates the XRD patterns for $FASnI_3$ and $FASnI_3$ with 10% of UA as an additive. For the $FASnI_3$ film, the XRD pattern contains peaks at 14.0°, 24.4°, 28.22°, 31.65°, and 40.37°, indicating an orthorhombic phase for $FASnI_3$. All these peaks prove that the $FASnI_3$ film is composed of random orientation grains [38]. The $FASnI_3$ film with UA has provided slightly more intense patterns, indicating better crystallinity in consistence with the absorption spectra. In addition, XRD patterns do not show remarkable changes in the curves after the addition of UA, which proves UA is not replaced into the Sn-perovskite lattice [39]. Fig. S2 compares the XRD spectrum for two kinds of films: (1) the combination of SnI_2 with SnF_2 and (2) a combination of SnI_2 mixed with SnF_2 and UA films. All films only showed the characteristics related to SnI_2 [40]. As shown, the peak intensity diminished in the second film. It can be attributed to the creation of SnY_2-UA complexes due to the Lewis acid-base adduct [41].

From the SEM cross-section, it can be found that the penetration of $FASnI_3$ in the porous alumina is not ideal and there are obvious holes in the filling. When the 10% UA content is added, it can be found that the filling conditions of aluminum oxide and titanium dioxide are very good, and the filling is complete without the existence of obvious holes. This pinhole-free and compact perovskite layers are useful for cell performance (Fig. 3). For a better understanding of the effect of UA on morphology, we compared the SEM image of the perovskite film with and without using UA (Fig. S3). It showed that adding UA has significant effects on the morphology of the perovskite film and led to the formation of a compact and pinhole-free film. It is attributed to a decrease in the crystal growth rate and happening uniform nucleation in UA + $FASnI_3$ films. However, when the amount of UA was increased to 15%, the perovskite film became much rougher than the perovskite film with 10%. UA.

The function of the UA additive on the oxidation of Sn^{2+} was examined via XPS measurements. As in Fig. 4a and 4b, the XPS spectra were deconvoluted into two sections involving Sn^{4+} and Sn^{2+} species in the binding energies of 486.6 eV and 486 eV, respectively. According to the fitting results, the $FASnI_3$ film involved much larger Sn^{4+} peaks than the $FASnI_3$ + UA film. This is because the amount of Sn^{4+} in the $FASnI_3$ film was much higher than in the $FASnI_3$ + UA film. Also, according to some previous studies, the amount of Sn^{4+} in $FASnI_3$ films is high [1]. In our study, the Sn^{2+} peak of the $FASnI_3$+ UA film was larger than the Sn^{4+} peak, but, in the $FASnI_3$ film, the Sn^{2+} peak was smaller than the Sn^{4+} Peak. It can, therefore, be concluded that UA can remarkably inhibit the oxidation of Sn^{2+} in perovskite layers. To investigate the charge dynamics of the fabricated films, normal photoluminescence (PL) spectroscopy was performed with samples that were assembled on glass substrates. Fig. 4c exhibits the steady-state PL spectra for the $FASnI_3$ and $FASnI_3$+UA samples. All the samples had emission peaks of about 895 nm. The PL intensity of reference film ($FASnI_3$) was lower than that of $FASnI_3$+UA, indicating higher non-radiative recombination losses for the charge carriers in $FASnI_3$ as a result of the free carriers captured in the defect sites. It was also found that the Sn^{2+} oxidation and the formation of Sn^{4+} could increase the non-radiative recombination and decrease the PL intensity. In addition, lower crystallinity could result in lower PL intensity in $FASnI_3$ [31,42].

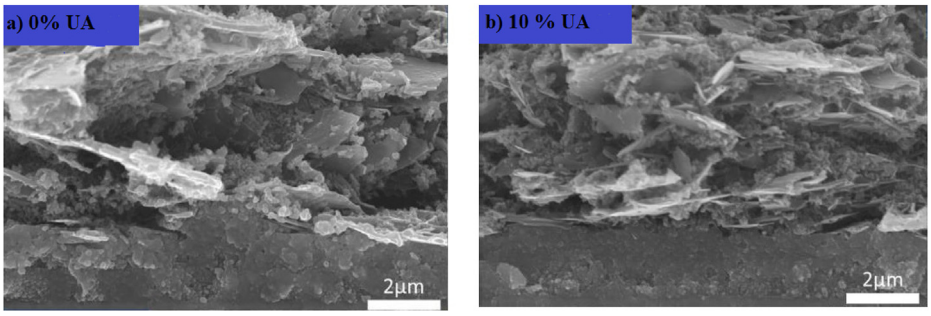

Fig. 3. SEM cross-sectional view of the $TiO_2/Al_2O_3/C$ structure of the device, a) without using UA, and b) after adding 10% UA.

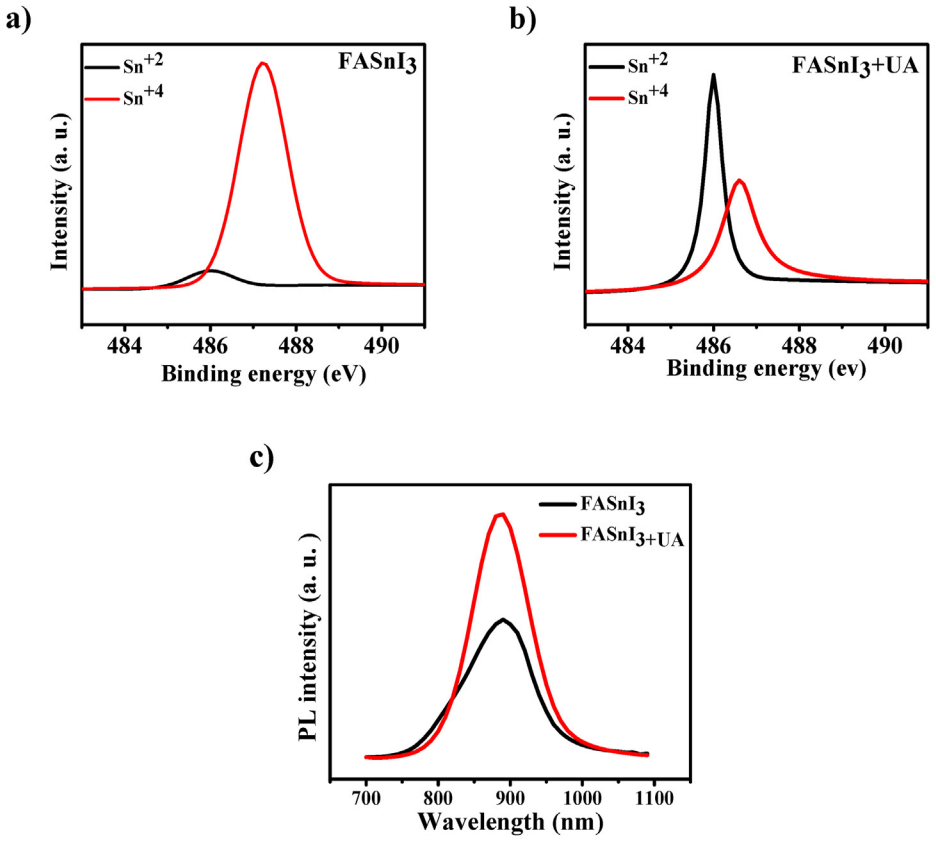

Fig. 4. XPS patterns to show distribution of Sn^{2+} and Sn^{4+} in samples a) $FASnI_3$, b) $FASnI_3$+ 10% UA. c) Photoluminescence of $FASnI_3$ and $FASnI_3$+ 10% UA.

Photocurrent-voltage (I–V) curves were recorded for different prepared devices. Fig. 5 illustrates these I–V curves, and Table 1 presents the photovoltaic parameters (V_{oc}, J_{sc}, FF (fill factor), and PCE) for the samples. As the results indicated, the Sn-based perovskite device prepared without using UA had lower performance, a PCE of 0.8%, and the photovoltaic parameters of V_{oc}: 146 mV, J_{sc}: 18.29 mA cm^{-2}, and FF: 30.14. However, in the device prepared with UA, there was an improved PCE of 1.2% along with the parameters J_{sc}: 22.36 mA cm^{-2}, V_{oc}: 189.5 mV, and FF: 28.1. Our results show remarkably improved V_{oc} and J_{sc} in the presence of UA. According to the XPS results, the improvement of PCE through the addition of UA can be ascribed to the retarded Sn^{2+} oxidation, which significantly inhibits the defect generation and decreases recombination. This is in accordance with PL findings. In addition,

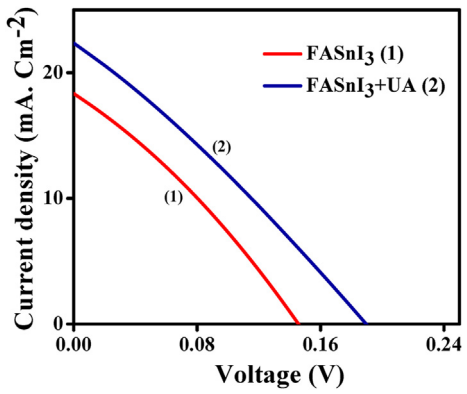

Fig. 5. J–V curves for the cells involving $FASnI_3$ (1) and $FASnI_3$+ 10% UA (2).

Table 1
Figures of merit for different devices.

Devices	J_{sc} (mA. Cm^{-2})	V_{oc} (V)	FF (%)	η (%)
$FASnI_3$	18.29	0.146	30.1	0.80
$FASnI_3$ + 10% UA	22.36	0.189	28.1	1.2

the improved photovoltaic parameters provide evidence for the noticeable decrease of defects and charge trapping cites because of the improvement in crystallites according to XRD, UV, and SEM results. Fig. S4 shows the stabilized power output powers of devices, $FASnI_3$ and $FASnI_3$ +UA, for 600 s. As can be seen, devices based on $FASnI_3$ +UA indicate better steady-state efficiency.

To evaluate PSCs, stability is an important factor to consider. For this reason, we investigated the UV absorption spectra for unencapsulated devices with $FASnI_3$ and $FASnI_3$ + UA 10% films after exposing them to ambient conditions (30% humidity) for 0, 3, and 6 h (Fig. S5. (a)). Other than our study, long-term stability was investigated for $FASnI_3$ + UA in GB after one week, two weeks, and one month (Fig. S5. (b)). All the UV spectra revealed that devices with UA would have better stability than those without UA. Moreover, we compared the XRD patterns of fresh and old (2 weeks in GB) perovskite films with 10% UA (Fig. S5. (c)). The devices with $FASnI_3$ rapidly decomposed to SnI_4 [21], but those with UA did not in two weeks. It brings one to the conclusion that UA additives not only decrease tin oxidation, but also protect perovskite structures against oxygen and moisture. Due to the structure of uric acid, this compound can stabilize the perovskite structure through hydrogen interactions and prevent further oxidation. Because it can reduce the electron density on iodide atoms and thus improve structural stability [43].

4. Conclusion

In this study, a natural antioxidant was used as an efficient additive to prevent Sn^{2+} oxidation in Sn PSCs with a carbon counter electrode. The screen-printed method was used to fabricate the cells, and then a perovskite solution containing UA was added to those cells. The results indicated that UA, an inexpensive and available antioxidant, is a suitable candidate with which to achieve better photovoltaic parameters and stability in $FASnI_3$ PSCs. The improvement is made through the reduction of Sn^{2+}oxidation to Sn^{4+}, a decrease of recombination, and the enhancement of crystallinity. Application of antioxidants to elevate the performance and stability in Sn−PSCs seems to be a noticeable strategy and an alternative procedure for the use of expensive additives. In this respect, it is more desirable to use antioxidants that have certain functional groups like OH^-, NH_2, or SO_3^-.

Funding

This research did not receive any specific grant.

Submission declaration and verification

All authors claimed that this article has not been published previously. Also, it is not under consideration for publication elsewhere. Its publication is approved by all authors and explicitly by the responsible authorities where the work was carried out. If this article is accepted, it will not be published elsewhere in the same form, in English or in any other language, including electronically without the written consent of the copyright holder.

CRediT authorship contribution statement

Hamideh Mohammadian-Sarcheshmeh: Writing - original draft. **Mohammad Mazloum-Ardakani:** Writing - review & editing. **Mohammad Rameez:** Conceptualization, Data curation, Formal analysis. **Saeed Shahbazi:** Conceptualization, Data curation, Formal analysis. **Eric Wei-Guang Diau:** Project administration, Resources.

Declaration of competing interest

The authors declare that they have no known competing financial interests or personal relationships that could have appeared to influence the work reported in this paper.

Acknowledgments

We are so thankful to Yazd University, Iran, and National Chiao Tung University, Hsinchu, Taiwan.

Appendix A. Supplementary data

Supplementary data to this article can be found online at https://doi.org/10.1016/j.jallcom.2020.156351.

References

[1] T. Krishnamoorthy, H. Ding, C. Yan, W.L. Leong, T. Baikie, Z. Zhang, M. Sherburne, S. Li, M. Asta, N. Mathews, Lead-free germanium iodide perovskite materials for photovoltaic applications, J. Mater. Chem. 3 (2015) 23829−23832.
[2] M. Lyu, J.-H. Yun, M. Cai, Y. Jiao, P.V. Bernhardt, M. Zhang, Q. Wang, A. Du, H. Wang, G. Liu, Organic−inorganic bismuth (III)-based material: a lead-free, air-stable and solution-processable light-absorber beyond organolead perovskites, Nano Research 9 (2016) 692−702.
[3] A.N. Usoltsev, M. Elshobaki, S.A. Adonin, L.A. Frolova, T. Derzhavskaya, P.A. Abramov, D.V. Anokhin, I.V. Korolkov, S.Y. Luchkin, N.N. Dremova, Polymeric iodobismuthates {[Bi_3 I_{10}]} and {[BiI_4]} with N-heterocyclic cations: promising perovskite-like photoactive materials for electronic devices, J. Mater. Chem. 7 (2019) 5957−5966.
[4] S.A. Adonin, L.A. Frolova, M.N. Sokolov, G. V Shilov, D. V Korchagin, V.P. Fedin, S.M. Aldoshin, K.J. Stevenson, P.A. Troshin, Antimony (V) complex halides: lead-free perovskite-like materials for hybrid solar cells, Adv.Energy Mater. 8 (2018) 1701140.
[5] T. Feurer, F. Fu, T.P. Weiss, E. Avancini, J. Löckinger, S. Buecheler, A.N. Tiwari, RbF post deposition treatment for narrow bandgap Cu (In, Ga) Se_2 solar cells, Thin Solid Films 670 (2019) 34−40.
[6] A.M. Kumar, I.J. Peter, K. Ramachandran, J. Mayandi, K. Jayakumar, Influence of Al-Cu doping on the efficiency of $BiFeO_3$ based perovskite solar cell (PSC), Mater. Today: Proceedings (2019) 1−4, https://doi.org/10.1016/j.matpr.2019.05.454.
[7] H. Li, R. Yang, C. Wang, Y. Wang, H. Chen, H. Zheng, D. Liu, T. Zhang, F. Wang, P. Gu, Corrosive behavior of silver electrode in inverted perovskite solar cells based on Cu: NiOx, IEEE. J.Photovoltaics 9 (2019) 1081−1085.
[8] N. Nicoara, R. Manaligod, P. Jackson, D. Hariskos, W. Witte, G. Sozzi, R. Menozzi, S. Sadewasser, Direct evidence for grain boundary passivation in Cu (In, Ga) Se_2 solar cells through alkali-fluoride post-deposition treatments, Nat. Commun. 10 (2019) 1−8.
[9] B. Saparov, F. Hong, J.-P. Sun, H.-S. Duan, W. Meng, S. Cameron, I.G. Hill, Y. Yan, D.B. Mitzi, Thin-film preparation and characterization of $Cs_3Sb_2I_9$: a lead-free layered perovskite semiconductor, Chem. Mater. 27 (2015) 5622−5632.
[10] T. Yokoyama, D.H. Cao, C.C. Stoumpos, T.-B. Song, Y. Sato, S. Aramaki, M.G. Kanatzidis, Overcoming short-circuit in lead-free $CH_3NH_3SnI_3$ perovskite solar cells via kinetically controlled gas−solid reaction film fabrication process, J. Phys. Chem. Lett. 7 (2016) 776−782.
[11] Q. Tai, J. Cao, T. Wang, F. Yan, Recent advances toward efficient and stable tin-based perovskite solar cells, EcoMat 1 (2019), e12004.
[12] X. Meng, T. Wu, X. Liu, X. He, T. Noda, Y. Wang, H. Segawa, L. Han, Highly reproducible and efficient FASnI3 perovskite solar cells fabricated with volatilizable reducing solvent, J. Phys. Chem. Lett. 11 (8) (2020) 2965−2971.
[13] M.H. Kumar, S. Dharani, W.L. Leong, P.P. Boix, R.R. Prabhakar, T. Baikie, C. Shi, H. Ding, R. Ramesh, M. Asta, Lead-free halide perovskite solar cells with high photocurrents realized through vacancy modulation, Adv. Mater. 26 (2014) 7122−7127.
[14] W. Liao, D. Zhao, Y. Yu, C.R. Grice, C. Wang, A.J. Cimaroli, P. Schulz, W. Meng, K. Zhu, R. Xiong, Lead-free inverted planar formamidinium tin triiodide perovskite solar cells achieving power conversion efficiencies up to 6.22%, Adv. Mater. 28 (2016) 9333−9340.
[15] Y. Dang, Y. Zhou, X. Liu, D. Ju, S. Xia, H. Xia, X. Tao, formation of hybrid perovskite tin iodide single crystals by top-seeded solution growth, Angew. Chem. Int. Ed. 55 (2016) 3447−3450.
[16] S.G. Mhaisalkar, W.L. Leong, C. Shi, P.P. Boix, H. Ding, M.H. Kumar, S. Dharani, R.R. Prabhakar, T. Baikie, R. Ramesh, Lead-free halide perovskite solar cells with high photocurrents realized through vacancy modulation, 2014.
[17] F. Hao, C.C. Stoumpos, P. Guo, N. Zhou, T.J. Marks, R.P.H. Chang, M.G. Kanatzidis, Solvent-mediated crystallization of $CH_3NH_3SnI_3$ films for heterojunction depleted perovskite solar cells, J. Am. Chem. Soc. 137 (2015) 11445−11452.
[18] S.J. Lee, S.S. Shin, Y.C. Kim, D. Kim, T.K. Ahn, J.H. Noh, J. Seo, S. Il Seok, Fabrication of efficient formamidinium tin iodide perovskite solar cells through SnF_2−pyrazine complex, J. Am. Chem. Soc. 138 (2016) 3974−3977.
[19] Z. Zhao, F. Gu, Y. Li, W. Sun, S. Ye, H. Rao, Z. Liu, Z. Bian, C. Huang, Mixed-organic-cation tin iodide for lead-free perovskite solar cells with an efficiency of 8.12%, Advanced Science 4 (2017) 1700204.
[20] T.M. Koh, T. Krishnamoorthy, N. Yantara, C. Shi, W.L. Leong, P.P. Boix, A.C. Grimsdale, S.G. Mhaisalkar, N. Mathews, Formamidinium tin-based perovskite with low E g for photovoltaic applications, J. Mater. Chem. 3 (2015) 14996−15000.
[21] E. Jokar, C.-H. Chien, A. Fathi, M. Rameez, Y.-H. Chang, E.W.-G. Diau, Slow surface passivation and crystal relaxation with additives to improve device performance and durability for tin-based perovskite solar cells, Energy Environ. Sci. 11 (2018) 2353−2362.
[22] Y. Liao, H. Liu, W. Zhou, D. Yang, Y. Shang, Z. Shi, B. Li, X. Jiang, L. Zhang, L.N. Quan, Highly oriented low-dimensional tin halide perovskites with enhanced stability and photovoltaic performance, J. Am. Chem. Soc. 139 (2017) 6693−6699.
[23] J. Kim, A. Ho-Baillie, S. Huang, Review of novel passivation techniques for efficient and stable perovskite solar cells, Solar RRL 3 (2019) 1800302.
[24] Q. Tai, X. Guo, G. Tang, P. You, T. Ng, D. Shen, J. Cao, C. Liu, N. Wang, Y. Zhu, Antioxidant grain passivation for air-stable tin-based perovskite solar cells, Angew. Chem. Int. Ed. 58 (2019) 806−810.
[25] H. Ban, Q. Sun, T. Zhang, H. Li, Y. Shen, M. Wang, Stabilization of inorganic $CsPb_{0.5}Sn_{0.5}I_2Br$ perovskite compounds by antioxidant tea polyphenol, Solar RRL (2019) 1900457.
[26] K.-M. Liu, D. Swann, P.-F. Lee, K.-W. Lam, Inhibition of oxidative degradation of hyaluronic acid by uric acid, Curr. Eye Res. 3 (1984) 1049−1053.
[27] K.J.A. Davies, A. Sevanian, S.F. Muakkassah-Kelly, P. Hochstein, Uric acid-iron ion complexes. A new aspect of the antioxidant functions of uric acid, Biochem. J. 235 (1986) 747−754.
[28] C.X.C. Santos, E.I. Anjos, O. Augusto, Uric acid oxidation by peroxynitrite: multiple reactions, free radical formation, and amplification of lipid oxidation,

Arch. Biochem. Biophys. 372 (1999) 285–294.
[29] V.V. Ramana, V.J. Thyagaraju, K.S. Sastrys, Chromium complexes of uric acid—synthesis, structure, and properties, J. Inorg. Biochem. 48 (1992) 85–93.
[30] M.M. Moawad, Complexation and thermal studies of uric acid with some divalent and trivalent metal ions of biological interest in the solid state, J. Coord. Chem. 55 (2002) 61–78.
[31] F. Wang, J. Ma, F. Xie, L. Li, J. Chen, J. Fan, N. Zhao, Organic cation-dependent degradation mechanism of organotin halide perovskites, Adv. Funct. Mater. 26 (2016) 3417–3423.
[32] A. Mei, X. Li, L. Liu, Z. Ku, T. Liu, Y. Rong, M. Xu, M. Hu, J. Chen, Y. Yang, A hole-conductor–free, fully printable mesoscopic perovskite solar cell with high stability, Science 345 (2014) 295–298.
[33] Y. Yang, J. Xiao, H. Wei, L. Zhu, D. Li, Y. Luo, H. Wu, Q. Meng, An all-carbon counter electrode for highly efficient hole-conductor-free organo-metal perovskite solar cells, RSC Adv. 4 (2014) 52825–52830.
[34] X. Li, M. Tschumi, H. Han, S.S. Babkair, R.A. Alzubaydi, A.A. Ansari, S.S. Habib, M.K. Nazeeruddin, S.M. Zakeeruddin, M. Grätzel, Outdoor performance and stability under elevated temperatures and long-term light soaking of triple-layer mesoporous perovskite photovoltaics, Energy Technol. 3 (2015) 551–555.
[35] A. Kay, M. Grätzel, Low cost photovoltaic modules based on dye sensitized nanocrystalline titanium dioxide and carbon powder, Sol. Energy Mater. Sol. Cell. 44 (1996) 99–117.
[36] Z. Ku, Y. Rong, M. Xu, T. Liu, H. Han, Full printable processed mesoscopic $CH_3NH_3PbI_3/TiO_2$ heterojunction solar cells with carbon counter electrode, Sci. Rep. 3 (2013) 3132.
[37] C.-Y. Chan, Y. Wang, G.-W. Wu, E.W.-G. Diau, Solvent-extraction crystal growth for highly efficient carbon-based mesoscopic perovskite solar cells free of hole conductors, J. Mater. Chem. 4 (2016) 3872–3878.
[38] F. Hao, C.C. Stoumpos, D.H. Cao, R.P.H. Chang, M.G. Kanatzidis, Lead-free solid-state organic–inorganic halide perovskite solar cells, Nat. Photon. 8 (2014) 489.
[39] H. Ban, Q. Sun, T. Zhang, H. Li, Y. Shen, M. Wang, Stabilization of inorganic $CsPb_{0.5}Sn_{0.5}I_2Br$ perovskite compounds by antioxidant tea polyphenol, Solar RRL 4 (2020) 1900457.
[40] C.S. Yoder, S. Shenk, R.W. Schaeffer, B. Chan, M. Molinaro, S. Morissey, C.H. Yoder, The synthesis, characterization, and Lewis acidity of SnI_2 and SnI_4, J. Chem. Educ. 74 (1997) 575.
[41] J.-W. Lee, H.-S. Kim, N.-G. Park, Lewis acid–base adduct approach for high efficiency perovskite solar cells, Acc. Chem. Res. 49 (2016) 311–319.
[42] D. Moghe, L. Wang, C.J. Traverse, A. Redoute, M. Sponseller, P.R. Brown, V. Bulović, R.R. Lunt, All vapor-deposited lead-free doped $CsSnBr_3$ planar solar cells, Nano Energy 28 (2016) 469–474.
[43] X. Meng, J. Lin, X. Liu, X. He, Y. Wang, T. Noda, T. Wu, X. Yang, L. Han, Highly stable and efficient $FASnI_3$-based perovskite solar cells by introducing hydrogen bonding, Adv. Mater. 31 (2019) 1903721.